

# Adaptive Polarized Waveform Design for Target Tracking Based on Sequential Bayesian Inference

Martin Hurtado, Tong Zhao, *Member, IEEE*, and Arye Nehorai, *Fellow, IEEE*

**Abstract**—In this paper, we develop an adaptive waveform design method for target tracking under a framework of sequential Bayesian inference. We employ polarization diversity to improve the tracking accuracy of a target in the presence of clutter. We use an array of electromagnetic (EM) vector sensors to fully exploit the polarization information of the reflected signal. We apply a sequential Monte Carlo method to track the target parameters, including target position, velocity, and scattering coefficients. This method has the advantage of being able to handle nonlinear and non-Gaussian state and measurement models. The measurements are the output of the sensor array; hence, the information about both the target and its environment is incorporated in the tracking process. We design a new criterion for selecting the optimal waveform one-step ahead based on a recursion of the posterior Cramér-Rao bound. We also derive an algorithm using Monte Carlo integration to compute this criterion and a suboptimal method that reduces the computation cost. Numerical examples demonstrate both the performance of the proposed tracking method and the advantage of the adaptive waveform design scheme.

**Index Terms**—Adaptive design, polarimetric radar, posterior Cramér-Rao bound, radar tracking, sequential Bayesian filter, waveform design.

## I. INTRODUCTION

ADAPTIVE design and processing of diverse waveforms are advanced technologies in radar signal processing used to achieve substantial improvements in sensing performance. Recent advances in sensor information processing and related hardware have motivated intense interest in adaptive waveform design. Specifically, advances in flexible digital waveform modulators make it feasible to implement pulse-to-pulse waveform selection capability in real time. Thus, there is a strong interest in fully exploiting the potential of radar systems through adaptive waveform design to obtain the highest possible performance level. In this paper we address the problem of adaptive polarized waveform design for tracking targets in the presence of clutter. The proposed scheme is derived under a framework of sequential Bayesian inference.

In a conventional active sensing system, parameters of the transmitted signal, e.g., waveform shape, polarization, and

frequency, are fixed, and the system is operated in an open loop independently of the environment. However, the target state evolves in time; furthermore, in some scenarios, the environment may also change, for example, with nonstationary clutter. If the fixed waveform does not match the operational scenario, the sensing system performance is severely limited. Thus, the purpose of our work is to adaptively design the transmitted waveform in response to the target's dynamic states and the environmental conditions in order to achieve a better tracking performance.

Another property of our waveform design scheme is that we employ the freedom provided by the polarization of the transmitted signal to design our system, whereas most waveform-design methods only the shape of the transmitted waveform is controlled [1], [2]. As we know, optimally selecting the polarization state of the transmitted waveform can mitigate multipath interference and improve the performance of the sensing system in detection, tracking, and target identification, as discussed in [3], references therein, and [4]–[7]. Therefore, by exploiting the polarimetric aspects of the reflected signals we can further improve the parameter estimation accuracy and the resolution of the targets.

A general procedure of adaptive waveform design for target tracking can be described as follows: 1) waveform-agile sensors transmit an optimally designed waveform and then take the measurements of the reflected signal from the target; 2) the tracker processes the received data and estimates the current states of the dynamic target parameters; 3) the tracking system also predicts the target states at the next time step; 4) the waveform-agile sensors optimally select the waveform parameters for the next transmitted signal according to a design criterion that depends on the current and predicted target states and the characteristics of the environment.

In this paper, we first propose a general framework for adaptive waveform design for target tracking in an active sensing system. This framework combines target tracking using sequential Bayesian filtering and optimal waveform selection. Most of the previous work on adaptive waveform design for target tracking [8]–[16] is derived under this framework, which also provides guidance for developing new technologies in this area.

We then propose a target dynamic state model and a statistical measurement model for target tracking. In the state model, we include the parameters of the scattering matrix; hence, we can track not only the target position and velocity but also its polarimetric aspects, which are useful, for example, for target identification [3]. In the measurement model, we include the polarization of the transmitted waveform and apply an electromagnetic (EM) vector-sensor array to receive the reflected signal. An EM vector sensor fully exploits the polarization information by

Manuscript received November 2, 2006; revised August 6, 2007. This work was supported in part by the Department of Defense under the Air Force Office of Scientific Research MURI Grant FA9550-05-0443, AFOSR Grant FA9550-05-1-0018, and by DARPA funding under NRL Grant N00173-06-1G006. The associate editor coordinating the review of this manuscript and approving it for publication was Prof. Steven M. Kay.

The authors are with the Department of Electrical and Systems Engineering, Washington University, St. Louis, MO 63130 USA (e-mail: mhurta3@ese.wustl.edu; tzhao3@ese.wustl.edu; nehorai@ese.wustl.edu).

Digital Object Identifier 10.1109/TSP.2007.909044

measuring all the components of the EM field [4], [5], and it has been shown that employing vector sensors improves the estimation of the signal direction of arrival (DOA) and the resolution of closely spaced signal arrivals [4], [17], [18]. We also extend the measurement model to consider more conventional polarimetric sensor arrays, e.g., tripole [19] and 2-D vector sensors [20].

Next, we develop a sequential (recursive) Bayesian filtering for target tracking and adaptive waveform design. Some work on adaptive waveform design for target tracking is presented in [8]–[16]. In [8] and [9], the state and measurement models are assumed to be linear and Gaussian; hence, a Kalman filter is used for target tracking, and the criteria of minimum mean-square tracking error and minimum validation gate volume are used for optimal waveform design. In [10] and [11], also assuming linear and Gaussian models, the concept of adaptive waveform selection is extended to interacting multiple model trackers looking one and two steps ahead. In [13]–[16], the methods are applied to a linear Gaussian state model and a nonlinear Gaussian measurement model, and the optimal waveform parameters are selected by minimizing a mean-square tracking error. A common characteristic in [8]–[16] is that the time delay and Doppler response of the matched filter are considered as the measurements. This procedure simplifies the modeling but decouples the measurements from the clutter. In [14], for example, data probabilistic association is used to account for the clutter effects; however, there is no clear relationship between the measurement's association probabilities and the clutter features. In our proposed approach, the measurements are the direct output of the polarimetric sensor array. Hence, we can incorporate into the tracking and waveform design algorithm information about the target and its environment in a more natural way, especially regarding their polarization aspects. Then, we track a target using a sequential Monte Carlo method (particle filter) that is suitable for nonlinear and non-Gaussian state and measurement models. In contrast with ordinary particle filtering methods, we consider that the potential dimension of state space can be large (we track the target position, velocity, and scattering parameters simultaneously), and we propose to use a Gibbs sampler that is a Markov chain Monte Carlo (MCMC) algorithm that allows successful solution of simulation problems for complex models.

We also develop a new criterion for selecting the optimal waveform one step ahead that is based on a posterior Cramér-Rao bound (PCRB). We adopt a recursive form to derive the PCRB. We employ a Monte Carlo integration method to calculate this criterion. In addition, we present a suboptimal criterion that reduces the computation cost with respect to the former waveform-selection rule. Note that according to sequential Bayesian framework, the proposed method can be extended to other criteria for adaptive waveform design. The motivations for using the PCRB here are as follows: 1) it is a lower bound for the mean-square error (MSE) of Bayesian estimation; 2) the calculation of the criterion can be integrated in the proposed sequential Monte Carlo tracking approach, hence decrease the computation complexity; 3) since the computation of the criterion is based on Bayesian inference, we do not need to know the specific value of the next measurements for its

calculation [in contrast with other work in [12]–[16] that uses MSE as a criterion]. Therefore, we increase the processing accuracy.

In Section II, we propose a general framework for an adaptive waveform design based on sequential Bayesian inference. In Section III, we derive a target dynamic state model and a statistical measurement model using an EM vector-sensor array. In Section IV, we develop a sequential Monte Carlo method to track the target. In Section V, we design a new criterion to optimally select the transmitted waveform based on posterior Cramér-Rao bounds. Numerical examples and conclusions are given in Sections VI and VII, respectively.

## II. SEQUENTIAL BAYESIAN FRAMEWORK FOR ADAPTIVE WAVEFORM DESIGN

The problem of waveform design consists of finding the signal parameters or selecting the waveforms that improve the system performance. In this section, we provide a general framework for adaptive waveform design based on sequential Bayesian inference. This framework is a combination of sequential Bayesian filtering for parameter estimation and optimal transmitted waveform design in active sensing systems.

This framework for adaptive waveform design includes four phases: 1) creation of a dynamic state model and a statistical measurement model; 2) belief prediction and update; 3) Bayesian state estimation; and 4) optimal waveform selection. They are described in details as follows.

1) *Dynamic State Model and Measurement Model*: To formulate a sequential Bayesian estimation, we first consider a state sequence  $\{\mathbf{x}_k, k \in \mathbb{N}\}$ ,  $\mathbf{x}_k \in \mathbb{R}^{n_x}$ , which is assumed to be an unobserved (hidden) Markov process with initial distribution  $p(\mathbf{x}_0)$ . The evolution of the state sequence is given by

$$\mathbf{x}_k = \mathbf{f}_k(\mathbf{x}_{k-1}, \mathbf{v}_{k-1}) \quad (1)$$

where  $\mathbf{f}_k : \mathbb{R}^{n_x} \times \mathbb{R}^{n_v} \rightarrow \mathbb{R}^{n_x}$  is a nonlinear function of the state;  $\{\mathbf{v}_k, k \in \mathbb{N}\}$  is a process noise sequence; and  $n_x$  and  $n_v$  are the dimensions of the state and process noise vectors, respectively. This state model represents our prior knowledge about, e.g., the underlying dynamic movement of a target.

We also have a sequence of measurements  $\{\mathbf{y}_k, k \in \mathbb{N}\}$ ,  $\mathbf{y}_k \in \mathbb{R}^{n_y}$ . These measurements are related to the current state vector via the observation equation:

$$\mathbf{y}_k = \mathbf{h}_k(\mathbf{x}_k, \mathbf{e}_k) \quad (2)$$

where  $\mathbf{h}_k : \mathbb{R}^{n_x} \times \mathbb{R}^{n_e} \rightarrow \mathbb{R}^{n_y}$  is a nonlinear function;  $\{\mathbf{e}_k, k \in \mathbb{N}\}$  is a measurement noise sequence; and  $n_y$  and  $n_e$  are the dimensions of the measurement and noise vectors, respectively.

2) *Belief Prediction and Update*: We denote by  $\mathbf{x}_{0:k} \triangleq \{\mathbf{x}_0, \dots, \mathbf{x}_k\}$  and  $\mathbf{y}_{1:k} \triangleq \{\mathbf{y}_1, \dots, \mathbf{y}_k\}$ , respectively, the state sequence and the observations up to  $k$ . Under the Bayesian inference framework, all relevant information about  $\mathbf{x}_{0:k}$  given observations  $\mathbf{y}_{1:k}$  can be obtained from the posterior probability density (also called *belief*)  $p(\mathbf{x}_{0:k}|\mathbf{y}_{1:k})$ . Therefore, our aim is to estimate recursively in time the distribution  $p(\mathbf{x}_{0:k}|\mathbf{y}_{1:k})$  and its associated features, including  $p(\mathbf{x}_k|\mathbf{y}_{1:k})$ .

In order to derive a recursive Bayesian inference process, we consider that the following conditional independent assumptions for a first-order hidden Markov process are satisfied.

A1: Conditioned on  $\mathbf{x}_k$ , the current measurements  $\mathbf{y}_k$  are independent of the past states  $\mathbf{x}_{0:k-1}$  and past measurement history  $\mathbf{y}_{1:k-1}$ , i.e.

$$p(\mathbf{y}_k | \mathbf{x}_{0:k}, \mathbf{y}_{1:k-1}) = p(\mathbf{y}_k | \mathbf{x}_k). \quad (3)$$

A2: Conditioned on  $\mathbf{x}_{k-1}$ , the current state  $\mathbf{x}_k$  is independent of the states  $\mathbf{x}_{0:k-2}$  and past measurement history  $\mathbf{y}_{1:k-1}$ , i.e.

$$p(\mathbf{x}_k | \mathbf{x}_{0:k-1}, \mathbf{y}_{1:k-1}) = p(\mathbf{x}_k | \mathbf{x}_{k-1}). \quad (4)$$

Based on these assumptions, we obtain recursive formulas to calculate the new belief  $p(\mathbf{x}_{0:k} | \mathbf{y}_{1:k})$  when the new measurements  $\mathbf{y}_k$  are available, as follows:

$$p(\mathbf{x}_{0:k} | \mathbf{y}_{1:k-1}) = p(\mathbf{x}_k | \mathbf{x}_{k-1}) p(\mathbf{x}_{0:k-1} | \mathbf{y}_{1:k-1}) \quad (5)$$

and

$$p(\mathbf{x}_{0:k} | \mathbf{y}_{1:k}) = \frac{p(\mathbf{y}_k | \mathbf{x}_k) p(\mathbf{x}_{0:k} | \mathbf{y}_{1:k-1})}{p(\mathbf{y}_k | \mathbf{y}_{1:k-1})} \quad (6)$$

where

$$p(\mathbf{y}_k | \mathbf{y}_{1:k-1}) = \int p(\mathbf{y}_k | \mathbf{x}_k) p(\mathbf{x}_{0:k} | \mathbf{y}_{1:k-1}) d\mathbf{x}_{0:k}. \quad (7)$$

For linear and Gaussian state and measurement models, the above equations become Kalman filters.

Equations (5) and (6) form a procedure for belief prediction and update in a recursive belief propagation. In the prediction stage (5), we use the probabilistic model of the state transition  $p(\mathbf{x}_k | \mathbf{x}_{k-1})$  and the measurement history  $\mathbf{y}_{1:k-1}$  to predict the prior probability density function (pdf) of the state at the  $k$ th time step. In the update stage (6), the current measurement  $\mathbf{y}_k$  (via the likelihood function  $p(\mathbf{y}_k | \mathbf{x}_k)$ ) is used to modify the prior density  $p(\mathbf{x}_k | \mathbf{y}_{1:k-1})$  to obtain the belief at the current time step.

3) *Bayesian State Estimation*: At the  $k$ th time step, after obtaining the current belief  $p(\mathbf{x}_k | \mathbf{y}_{1:k})$ , we can obtain an optimal estimate of the current state  $\mathbf{x}_k$ . In target tracking, this estimate can be used to determine the current target states (e.g., position and velocity) and environment parameters. Under the Bayesian framework, the estimate is calculated by optimizing a utility function. For example, when we apply a minimum-mean-squared error (MMSE) criterion, the estimate is the mean of the belief  $p(\mathbf{x}_k | \mathbf{y}_{1:k})$ .

4) *Optimal Waveform Selection*: In optimal waveform selection, we use the information from the current belief  $p(\mathbf{x}_k | \mathbf{y}_{1:k})$ , together with the state transition distribution and measurement model, to optimally select the waveform one step ahead in response to the target state and the environmental situation. Hence, we can achieve the best possible sensing performance.

To derive a mathematical formulation for optimal waveform selection, we first create a utility function according to certain criteria that represent the sensing performance; then, we determine the parameters for the next transmitted waveform by optimizing (e.g., maximizing) this utility function. We denote by

$J(\cdot)$  the utility function,  $\boldsymbol{\theta}_{k+1}$  the waveform parameters at the  $(k+1)$ th time step, and  $\mathbf{y}_{k+1}(\boldsymbol{\theta}_{k+1})$  the measurements at the  $(k+1)$ th time step. At the current time step  $k$ , we select the next transmitted waveform  $\boldsymbol{\theta}_{k+1}^*$  to be

$$\boldsymbol{\theta}_{k+1}^* = \arg \max_{\boldsymbol{\theta}_{k+1} \in \Theta} J[p(\mathbf{x}_{k+1} | \mathbf{y}_{1:k}, \mathbf{y}_{k+1}(\boldsymbol{\theta}_{k+1}))] \quad (8)$$

where  $\Theta$  denotes the set of the allowed values for  $\boldsymbol{\theta}_{k+1}$  or a library of possible waveforms.

We note that the former utility function is related to the belief at the  $(k+1)$ th time step. In order to determine this belief, we need the measurements  $\mathbf{y}_{k+1}$ , which are not available at the current time step  $k$ . Therefore, we compute the utility function  $J(\cdot)$  by marginalizing out the particular value of  $\mathbf{y}_{k+1}$ . We observe that for any given  $\mathbf{y}_{k+1}$ , we obtain a particular value for  $J(\cdot)$  acting on the new belief  $p(\mathbf{x}_{k+1} | \mathbf{y}_{1:k}, \mathbf{y}_{k+1}(\boldsymbol{\theta}_{k+1}))$ . Now for each waveform parameter  $\boldsymbol{\theta}_{k+1}$  we consider the set of all values of  $J(\cdot)$  for different values of  $\mathbf{y}_{k+1}$ . Possibilities for summarizing the set of values of  $J(\cdot)$  by a single quantity include the average, the worst, or the best case [21]. For example, if we use the average as a utility, the next transmitted waveform is selected by

$$\boldsymbol{\theta}_{k+1}^* = \arg \max_{\boldsymbol{\theta}_{k+1} \in \Theta} \mathbb{E}_{\mathbf{y}_{k+1} | \mathbf{y}_{1:k}} \{J[p(\mathbf{x}_{k+1} | \mathbf{y}_{1:k}, \mathbf{y}_{k+1}(\boldsymbol{\theta}_{k+1}))]\} \quad (9)$$

where  $\mathbb{E}_{\mathbf{y}_{k+1} | \mathbf{y}_{1:k}} \{\cdot\}$  represents the average over the set of new belief weighted by  $p(\mathbf{y}_{k+1} | \mathbf{y}_{1:k})$ .

We note that many tracking applications require fast real-time processing. The tradeoff between performance and computation cost should be considered when choosing the utility function  $J(\cdot)$ .

### III. TARGET DYNAMIC STATE MODEL AND MEASUREMENT MODEL

In this section, we first create a dynamic state model for target tracking. Based on this model, we can track the target position, velocity, and scattering coefficients. We then derive a measurement model that is the output of the receiver sensor array. This model provides a natural way of incorporating the polarimetric aspects of the target and clutter into the tracking filter.

#### A. Target Dynamic State Model

In our state model, we include the target scattering coefficients that are important, for example, for target identification and classification [3]. We denote by  $S_t$  the complex scattering matrix representing the polarization change of the transmit signal upon its reflection on the target:

$$S_t = \begin{bmatrix} s_{hh} & s_{hv} \\ s_{vh} & s_{vv} \end{bmatrix}. \quad (10)$$

The variables  $s_{hh}$  and  $s_{vv}$  are copolar scattering coefficients, whereas  $s_{hv}$  and  $s_{vh}$  are cross-polar coefficients. For the monostatic radar case,  $s_{hv} = s_{vh}$ .

The scattering matrix of the target can be written in terms of the radar polarization basis as [22]

$$S_t = R^T S_d R \quad (11)$$

where

- $R$  is a unitary transformation matrix from the target eigenbasis to the radar basis

$$R = \begin{bmatrix} \cos \vartheta & \sin \vartheta \\ -\sin \vartheta & \cos \vartheta \end{bmatrix} \cdot \begin{bmatrix} \cos \epsilon & j \sin \epsilon \\ j \sin \epsilon & \cos \epsilon \end{bmatrix} \quad (12)$$

where  $\vartheta$  is the orientation angle of the target eigenbasis around the line of sight and relative to the radar ( $-90^\circ \leq \vartheta \leq 90^\circ$ ), and  $\epsilon$  is the ellipticity of the target ( $-45^\circ \leq \epsilon \leq 45^\circ$ ).

- $S_d$  is a diagonal matrix representing the target scattering matrix in its eigenpolarization basis

$$S_d = m e^{j\varrho} \begin{bmatrix} e^{j2\nu} & 0 \\ 0 & \tan^2 \gamma e^{-j2\nu} \end{bmatrix} \quad (13)$$

where  $m$  is the maximum target amplitude;  $\varrho$  is the absolute phase of the scattering matrix ( $-180^\circ \leq \varrho \leq 180^\circ$ );  $\nu$  is called the skip angle, which is associated with the depolarization of the reflected signal ( $-45^\circ \leq \nu \leq 45^\circ$ ); and  $\gamma$  is called the characteristic angle, representing the ability of the target to polarize an incident unpolarized field ( $0^\circ \leq \gamma \leq 45^\circ$ ) [3]. These four parameters  $\{m, \varrho, \nu, \gamma\}$  do not change with the target orientation about the line of sight; hence, they are called invariant parameters. The decomposition of the scattering matrix for the non-reciprocal case (i.e.  $s_{hv} \neq s_{vh}$ ) can be found in [23].

Then, we represent the target state at the  $k$ th time step as

$$\mathbf{x}_k = [\boldsymbol{\rho}_k^T, \mathbf{s}_k^T]^T \quad (14)$$

where  $\boldsymbol{\rho}_k = [x_k, y_k, z_k, \dot{x}_k, \dot{y}_k, \dot{z}_k]^T$  includes the target position and velocity at the  $k$ th time step in a Cartesian coordinate system, and  $\mathbf{s}_k = [\vartheta_k, \epsilon_k, m_k, \varrho_k, \nu_k, \gamma_k]^T$  represents the target scattering parameters.

We assume that: 1) the target movement is characterized by a constant velocity and random acceleration; 2) the target scattering parameters are nearly constant and have random rate of change; and 3) the position and velocity are statistically independent of the scattering coefficients. Then, we obtain a linear target dynamic state model given by

$$\mathbf{x}_k = F \mathbf{x}_{k-1} + \mathbf{v}_{k-1} = \begin{bmatrix} F_\rho & \mathbf{0} \\ \mathbf{0} & F_s \end{bmatrix} \mathbf{x}_{k-1} + \mathbf{v}_{k-1} \quad (15)$$

where

- $F_\rho$  is the transition matrix for states  $\boldsymbol{\rho}$  as

$$F_\rho = \begin{bmatrix} I_3 & T_{\text{PRI}} I_3 \\ \mathbf{0} & I_3 \end{bmatrix} \quad (16)$$

where  $I_n$  denotes the identity matrix of size  $n$ , and  $T_{\text{PRI}}$  is the pulse repetition interval (PRI).  $F_s = I_6$  is the transition matrix for state  $\mathbf{s}$ .

- $\mathbf{v}_k$  is the independent process noise, representing the uncertainty about the state model, and is assumed to be zero-mean Gaussian distributed with covariance matrix  $Q$

$$Q = \begin{bmatrix} Q_\rho & \mathbf{0} \\ \mathbf{0} & Q_s \end{bmatrix} \quad (17)$$

where  $Q_\rho$  and  $Q_s$  denote the covariance matrices for the target acceleration and rate of change of the scattering parameters [24], see (18) at the bottom of the page, and  $q_\rho$  and  $q_s$  are constants.

In this state model, the assumption that the target scattering coefficients vary slowly is suitable for a situation in which the target is far away from the sensor array and the target position change during the tracking period is not large compared with the distance between the target and the sensor array.

In general, the dynamic model for the scattering coefficients is a nonlinear function with respect to other states; hence, the target dynamic state model will be nonlinear. In some cases, it is difficult even to determine a closed-form dynamic transition model for the scattering coefficients. One solution is to assume the state transition density  $p(\mathbf{s}_{k+1}|\mathbf{s}_k)$  to be a uniform distribution centered at  $\mathbf{s}_k$  with a radius equal to the possible maximum value of the change of the scattering coefficients during  $T_{\text{PRI}}$ . That is, we do not provide any prior information about the change of  $\mathbf{s}_k$  except that  $\mathbf{s}_{k+1}$  will be within a certain range.

## B. Statistical Measurement Model

We consider a target characterized by azimuth  $\phi$ , elevation  $\psi$ , range  $r$ , Doppler shift  $\omega_D$ , and scattering matrix  $S_t$ . These parameters are related to the states  $\mathbf{x}$  in (14). To uniquely identify the polarimetric aspects of a target, polarization diversity is required and the complete EM information of the signal reflected from the target has to be processed [5]. To provide these measurements, we employ an array of EM vector sensors [4] as the receiver, where each sensor measures the six components of the

$$Q_\rho = q_\rho \begin{bmatrix} T_{\text{PRI}}^4/4 & 0 & 0 & T_{\text{PRI}}^3/2 & 0 & 0 \\ 0 & T_{\text{PRI}}^4/4 & 0 & 0 & T_{\text{PRI}}^3/2 & 0 \\ 0 & 0 & T_{\text{PRI}}^4/4 & 0 & 0 & T_{\text{PRI}}^3/2 \\ T_{\text{PRI}}^3/2 & 0 & 0 & T_{\text{PRI}}^2 & 0 & 0 \\ 0 & T_{\text{PRI}}^3/2 & 0 & 0 & T_{\text{PRI}}^2 & 0 \\ 0 & 0 & T_{\text{PRI}}^3/2 & 0 & 0 & T_{\text{PRI}}^2 \end{bmatrix} \quad (18)$$

$$Q_s = q_s T_{\text{PRI}}^2 I_6$$

EM field (three electric and three magnetic components of the received signal). In Section III-B-1, we briefly consider the application of more traditional sensors, such as tripoles [19] and 2-D sensors [20].

Consider an array of  $M$  vector sensors receiving the signal returns from a target. The complex envelope of the measurements can be expressed as

$$\mathbf{y}(t) = A(\phi, \psi) S_t \boldsymbol{\xi}(t - \tau) e^{j\omega_D t} + \mathbf{e}(t), \quad t = t_1, \dots, t_N \quad (19)$$

where the following is noted.

- The matrix  $A(\phi, \psi) = \mathbf{p}(\phi, \psi) \otimes V(\phi, \psi)$  is the array response, where  $\otimes$  is the Kronecker product;  $[\phi, \psi]^T$  is the bearing angle vector;  $\mathbf{p}(\phi, \psi) = [e^{j2\pi\mathbf{u}^T \mathbf{r}_1 / \lambda}, \dots, e^{j2\pi\mathbf{u}^T \mathbf{r}_M / \lambda}]^T$  represents the phase of the planewave arriving from the direction given by the vector  $\mathbf{u} = [\cos \phi \cos \psi, \sin \phi \cos \psi, \sin \psi]^T$  at the position  $\mathbf{r}_m$  of the  $m$ th sensor ( $m = 1, \dots, M$ );  $\lambda$  is the signal wavelength; and  $V(\phi, \psi)$  is the response of a single vector sensor given by [4]

$$V(\phi, \psi) = \begin{bmatrix} -\sin \phi & -\cos \phi \sin \psi \\ \cos \phi & -\sin \phi \sin \psi \\ 0 & \cos \psi \\ -\cos \phi \sin \psi & \sin \phi \\ -\sin \phi \sin \psi & -\cos \phi \\ \cos \psi & 0 \end{bmatrix}. \quad (20)$$

- The polarized transmit wave  $\boldsymbol{\xi}(t)$  is a narrowband signal that can be represented by a complex vector [3], [4]

$$\boldsymbol{\xi}(t) = \begin{bmatrix} \xi_h(t) \\ \xi_v(t) \end{bmatrix} = g(t) Q(\alpha) \mathbf{w}(\beta) \quad (21)$$

where

$$Q(\alpha) = \begin{bmatrix} \cos \alpha & \sin \alpha \\ -\sin \alpha & \cos \alpha \end{bmatrix}, \quad \mathbf{w}(\beta) = \begin{bmatrix} \cos \beta \\ j \sin \beta \end{bmatrix}. \quad (22)$$

Angles  $\alpha$  and  $\beta$  are the orientation and ellipticity of the polarization ellipse. The function  $g(t)$  represents the scalar complex envelope of the transmitted pulse. The time delay  $\tau = 2r/c$ , where  $r$  is the distance from the target to the sensor array and  $c$  is the wave propagation velocity.

- The vector  $\mathbf{e}(t)$  is the additive noise corrupting the radar measurements; it represents the thermal noise at the sensors and the reflections from the clutter (target environment).
- $N$  denotes the number of samples during the pulse repetition interval  $T_{\text{PRI}}$ .

Since  $\boldsymbol{\xi}(t)$  is the transmitted signal, the waveform design problem consists of selecting the envelope  $g(t)$  and the polarization angles  $\alpha$  and  $\beta$  in (21). We denote these waveform parameters by  $\boldsymbol{\theta}$ .

It can be verified that the relationship between the target parameters  $[\phi, \psi, r, \omega_D, S_t]$  and the states  $\mathbf{x} = [\boldsymbol{\rho}^T, \mathbf{s}^T]^T$  is given by

$$\phi = \arctan\left(\frac{y}{x}\right) \quad (23a)$$

$$\psi = \arctan\left(\frac{z}{\sqrt{x^2 + y^2}}\right) \quad (23b)$$

$$r = \sqrt{x^2 + y^2 + z^2} \quad (23c)$$

$$\omega_D = \frac{2\omega_c}{c} \frac{\dot{x}x + \dot{y}y + \dot{z}z}{\sqrt{x^2 + y^2 + z^2}} \quad (23d)$$

$$S_t = S_t(\mathbf{s}) \quad (23e)$$

where  $\omega_c$  is the carrier frequency, and the relation between  $S_t$  and  $\mathbf{s}$  is given in (11)–(13). When we insert (23) into the measurement model (19), we observe a nonlinear relationship between measurements  $\mathbf{y}(t)$  and state  $\mathbf{x}$ . We write this nonlinear relationship at the  $k$ th time step as

$$\mathbf{y}_k(t) = \tilde{\mathbf{h}}(t, \mathbf{x}_k; \boldsymbol{\theta}_k) + \mathbf{e}_k(t) \quad (24)$$

where

$$\tilde{\mathbf{h}}(t, \mathbf{x}; \boldsymbol{\theta}) = A(\phi, \psi) S_t \boldsymbol{\xi}(t - \tau) e^{j\omega_D t}, \quad t = t_1, \dots, t_N. \quad (25)$$

When we lump  $\{\mathbf{y}_k(t), t = t_1, \dots, t_N\}$  together into a vector, we obtain the following as measurement model:

$$\mathbf{y}_k = \begin{bmatrix} \mathbf{y}_k(t_1) \\ \vdots \\ \mathbf{y}_k(t_N) \end{bmatrix} = \begin{bmatrix} \tilde{\mathbf{h}}(t_1, \mathbf{x}_k; \boldsymbol{\theta}_k) \\ \vdots \\ \tilde{\mathbf{h}}(t_N, \mathbf{x}_k; \boldsymbol{\theta}_k) \end{bmatrix} + \begin{bmatrix} \mathbf{e}_k(t_1) \\ \vdots \\ \mathbf{e}_k(t_N) \end{bmatrix} = \mathbf{h}(\mathbf{x}_k; \boldsymbol{\theta}_k) + \mathbf{e}_k. \quad (26)$$

1) *Model Extension to Other Vector Sensors:* The above measurement model is based on the application of EM vector sensors to provide polarimetric information of the reflected signal. This model can also be extended to other polarimetric sensors by generalizing the matrix response of the vector sensor as

$$\tilde{V}(\phi, \psi) = \Upsilon(\phi, \psi) \Omega V(\phi, \psi) \quad (27)$$

where  $V(\phi, \psi)$  is given in (20) and  $\Upsilon(\phi, \psi)$  is a diagonal matrix whose  $l$ th diagonal entry is  $[\Upsilon(\phi, \psi)]_{ll} = e^{j2\pi\mathbf{u}^T \mathbf{q}_l / \lambda}$ , for  $l = 1, \dots, 6$ . This matrix provides the phase shift between the vector-sensor center and the position  $\mathbf{q}_l$  of the  $l$ th component.  $\Omega$  is a  $6 \times 6$  matrix whose entries are “0” or “1.” It has only one “1” per row, indicating the EM field measured by the  $l$ th sensor component. Equation (27) represents a distributed EM vector sensor [17] in which the components are not collocated. For the case of the collocated vector sensor [as the EM vector sensor in (20)], the matrices  $\Upsilon$  and  $\Omega$  are the identity matrix  $I_6$ . Equation (27) can represent the tripole and 2-D sensors by redefining matrix  $\Omega$  as

$$\Omega_{\text{tripole}} = \begin{bmatrix} 1 & 0 & 0 & 0 & 0 & 0 \\ 0 & 1 & 0 & 0 & 0 & 0 \\ 0 & 0 & 1 & 0 & 0 & 0 \\ 1 & 0 & 0 & 0 & 0 & 0 \\ 0 & 1 & 0 & 0 & 0 & 0 \\ 0 & 0 & 1 & 0 & 0 & 0 \end{bmatrix}$$

$$\Omega_{2D} = \begin{bmatrix} 1 & 0 & 0 & 0 & 0 & 0 \\ 0 & 0 & 1 & 0 & 0 & 0 \\ 1 & 0 & 0 & 0 & 0 & 0 \\ 0 & 0 & 1 & 0 & 0 & 0 \\ 1 & 0 & 0 & 0 & 0 & 0 \\ 0 & 0 & 1 & 0 & 0 & 0 \end{bmatrix}. \quad (28)$$

We note that EM vector sensors are expected to have constant performance in all directions and polarizations of the received signal since they measure all the components of the EM field [4]. On the other hand, to achieve good performance, 2-D sensors have to be steered using a mechanical device or a sensor array combined with beamforming techniques. Although tripoles measure the complete electric information of the received signal, we have shown in [18] that their performance on the estimation of direction-of-arrival parameters depends on the signal polarization and azimuth.

2) *Polarimetric Clutter Model*: The measurement noise  $\mathbf{e}(t)$  represents not only the thermal noise at the sensors of the receiver but also the reflections from the environment surrounding or behind the target. We aim to represent by this model the clutter reflections, for example, in the case for which a target flies above a sea or land surface.

It is well known that the clutter response is highly dependent on the transmit signal polarization [3], [25]. Conventional clutter models represent the term  $\mathbf{e}(t)$  in (19) with a random vector and apply training data to estimate its distribution parameters [26], [27]. In an adaptive polarized waveform system, training data must be recorded for all possible polarizations used by the transmitter, but this modeling procedure becomes highly inefficient. Instead, we propose a new polarimetric clutter model that explicitly accounts for the polarization of the illuminating signal, and only the clutter scattering coefficients are represented by a random vector. For estimating the statistical parameters of this random vector, training data recorded with simple two different polarized pulses are required [5]. In [28], we applied the former model for a radar detection problem and showed good performance using real radar data compared with detectors designed for other clutter models, such as compound-Gaussian and Weibull distributions.

The transmit signal illuminates both the target and the clutter, and their reflections are recorded by the same receiver. Hence, we propose a noise model, similar to measurement model (19), as

$$\mathbf{e}(t) = A(\phi_0, \psi_0) S_c \boldsymbol{\xi}(t - \tau_0) + \mathbf{n}(t), \quad t = t_1, \dots, t_N \quad (29)$$

where  $\mathbf{n}(t)$  is the additive thermal noise and  $S_c$  is the scattering matrix of the clutter. The angles  $[\phi_0, \psi_0]$  are the direction in which the radar beam is been steered, which might be different from the target angles. The clutter delay  $\tau_0$  is related to the average clutter position, and it may also differ from the target delay. For our cases of interest, we consider that the clutter does not introduce Doppler shift; i.e. the clutter velocity can be neglected when compared with the target velocity. The clutter

scattering coefficients are random variables because they represent the reflections from many incoherent point scatterers constituting the clutter. Following the model in [5], (29) can be rearranged to express the clutter scattering coefficients in a vector:

$$\mathbf{e}(t) = A(\phi_0, \psi_0) \boldsymbol{\xi}(t - \tau_0) \bar{S}_c + \mathbf{n}(t), \quad t = t_1, \dots, t_N \quad (30)$$

where

$$\boldsymbol{\xi}(t) = \begin{bmatrix} \xi_h(t) & 0 & \xi_v(t) \\ 0 & \xi_v(t) & \xi_h(t) \end{bmatrix} \quad (31)$$

and

$$\bar{S}_c = [s_{hh}^c, \quad s_{vv}^c, \quad s_{hv}^c]^T \quad (32)$$

where the variables  $s^c$  are the scattering coefficients of the clutter.

We assume that the thermal noise and the clutter scattering coefficients can be modeled as

$$\mathbf{n}(t) \sim \mathcal{CN}(0, \sigma^2 I_{6M}), \quad \bar{S}_c \sim \mathcal{CN}(0, \Sigma_c) \quad (33)$$

where  $\sigma^2$  is the noise power, and the clutter covariance matrix can be parameterized as [5]

$$\Sigma_c = \begin{bmatrix} \sigma_p^2 Q(\vartheta_c) \mathbf{w}(\epsilon_c) \mathbf{w}(\epsilon_c)^H Q(\vartheta_c) + \sigma_u^2 I_2 & 0 \\ 0 & p_x \end{bmatrix} \quad (34)$$

where  $\sigma_p^2$  and  $\sigma_u^2$  are the power of the polarized and unpolarized components of the clutter,  $\vartheta_c$  and  $\epsilon_c$  are the orientation and ellipticity angles of the clutter, matrix  $Q(\cdot)$  and vector  $\mathbf{w}(\cdot)$  are defined as in (22), and  $p_x$  is the power of the cross-polarized component of the clutter.

3) *Polarized Waveform Structure*: The design of the polarized waveform involves selecting the parameters of the signal envelope  $g(t)$  and its polarization in (21). Here, we consider as an example a linear frequency modulated (LFM) pulse with Gaussian envelope, which is defined as

$$g(t) = (\pi\eta^2)^{-1/4} \exp \left[ - \left( \frac{1}{2\eta^2} - jb \right) t^2 \right] \quad (35)$$

where  $\eta$  is the pulse length and  $b$  is the frequency sweep rate. The signal bandwidth is  $BW = 7.4\eta b$  [13]. Then, we propose to use the following scheme of polarized waveform [7]:

$$\boldsymbol{\xi}(t) = \sum_{l=0}^{L-1} g(t - lT_{\text{EPL}}) Q(\alpha_l) \mathbf{w}(\beta_l) \quad (36)$$

where  $L$  is the number of transmitted LFM pulses and  $T_{\text{EPL}} = 7.4\eta$  is the effective pulse length [13]. Under this scheme, the waveform parameters are  $\boldsymbol{\theta} = [\eta, b, \alpha_0, \beta_0, \dots, \alpha_{L-1}, \beta_{L-1}]^T$ .

Note that if the scattering matrix is completely unknown, at least two pulses with different polarization should be transmitted, i.e.  $L > 0$ , to uniquely identify  $S_t$ .

#### IV. TARGET TRACKING USING SEQUENTIAL MONTE CARLO METHODS

In this section, we develop a target-tracking method based on the proposed dynamic state model (15) and the statistical measurement model (26). Since these models are nonlinear, we propose a sequential Monte Carlo method (particle filter), which is

based on point mass representation of probability densities and is powerful for solving nonlinear and non-Gaussian Bayesian inference problems.

In contrast with the ordinary sequential Monte Carlo methods, in our proposed approach we adopt a Gibbs sampler to draw samples from an importance sampling function [29] through which we can handle the potentially large dimension of a state vector. We first describe the ordinary sequential importance sampling (SIS) particle filter and then we discuss the use of other possible importance sampling functions.

#### A. Sequential Importance Sampling Particle Filter

The sequential Monte Carlo method is a technique for implementing a recursive Bayesian filter by Monte Carlo simulations [29]–[35]. The key idea is to represent the required posterior density function by a set of random samples with associated weights and to compute estimates based on these samples and weights.

Let  $\{\mathbf{x}_{0:k}^{(i)}, w_k^{(i)}, i = 1, \dots, N_s\}$  denote a random measure that characterizes the belief  $p(\mathbf{x}_{0:k}|\mathbf{y}_{1:k})$ , where  $\{\mathbf{x}_{0:k}^{(i)}, i = 1, \dots, N_s\}$  is a set of support points with associated weights  $\{w_k^{(i)}, i = 1, \dots, N_s\}$ . Then, the belief at the  $k$ th time step can be approximated as

$$p(\mathbf{x}_{0:k}|\mathbf{y}_{1:k}) \approx \sum_{i=1}^{N_s} w_k^{(i)} \delta(\mathbf{x}_{0:k} - \mathbf{x}_{0:k}^{(i)}) \quad (37)$$

where the weights are chosen using the principle of importance sampling [29]. Let  $\{\mathbf{x}_{0:k}^{(i)}, i = 1, \dots, N_s\}$  be samples that are easily generated from a proposal importance density function  $q(\mathbf{x}_{0:k}^{(i)}|\mathbf{y}_{1:k})$ . Then, the weights in (37) are given by [34]

$$w_k^{(i)} \propto \frac{p(\mathbf{x}_{0:k}^{(i)}|\mathbf{y}_{1:k})}{q(\mathbf{x}_{0:k}^{(i)}|\mathbf{y}_{1:k})}. \quad (38)$$

For a sequential filtering case where only  $p(\mathbf{x}_k|\mathbf{y}_{1:k})$  is required at each time step, we can choose the importance density  $q(\cdot)$  such that we obtain a weight update equation [35]:

$$w_k^{(i)} \propto w_{k-1}^{(i)} \frac{p(\mathbf{y}_k|\mathbf{x}_k^{(i)})p(\mathbf{x}_k^{(i)}|\mathbf{x}_{k-1}^{(i)})}{q(\mathbf{x}_k^{(i)}|\mathbf{x}_{k-1}^{(i)}, \mathbf{y}_k)} \quad (39)$$

and the belief  $p(\mathbf{x}_k|\mathbf{y}_{1:k})$  can be approximated as

$$p(\mathbf{x}_k|\mathbf{y}_{1:k}) \approx \sum_{i=1}^{N_s} w_k^{(i)} \delta(\mathbf{x}_k - \mathbf{x}_k^{(i)}) \quad (40)$$

where  $\{\mathbf{x}_k^{(i)}, i = 1, \dots, N_s\}$  are sampled from the importance density  $q(\mathbf{x}_k|\mathbf{x}_{k-1}^{(i)}, \mathbf{y}_k)$ .

#### B. Gibbs Sampling-Based Particle Filter

Considering our target tracking problem, from the dynamic state model (15) we observe that if we want to track the target position, velocity, and scattering coefficients simultaneously, the dimension of the state space is large. Drawing samples directly from the importance density  $q(\mathbf{x}_k|\mathbf{x}_{k-1}^{(i)}, \mathbf{y}_k)$  is typically inefficient. Hence, we apply a Markov chain Monte Carlo (MCMC) method, a class of iterative simulation-based

methods, to sample from the importance density. MCMC methods are a set of procedures that enable the successful solution of simulation problems for more complex models [31], [32]. The basic idea of MCMC methods is to simulate an ergodic Markov chain whose samples are asymptotically distributed according to a desired density function. In our work, we adopt a classical MCMC algorithm—the Gibbs sampler. Given state  $\boldsymbol{\theta}$ , the Gibbs sampler consists of first defining a partition of the components of  $\boldsymbol{\theta}$  as  $\boldsymbol{\theta}_1, \dots, \boldsymbol{\theta}_p$  ( $p \leq \dim(\boldsymbol{\theta})$ ), and then sampling successively from the full conditional distributions  $p(\boldsymbol{\theta}_l|\boldsymbol{\theta}_{-l})$ , where  $\boldsymbol{\theta}_{-l} \triangleq (\boldsymbol{\theta}_1, \dots, \boldsymbol{\theta}_{l-1}, \boldsymbol{\theta}_{l+1}, \dots, \boldsymbol{\theta}_p)$ .

In our developed particle filter, we choose the importance density to be the transitional prior  $p(\mathbf{x}_k|\mathbf{x}_{k-1}^{(i)})$ ,  $i = 1, \dots, N_s$ . We adopt the above Gibbs sampling and propose the following method to draw samples from  $p(\mathbf{x}_k|\mathbf{x}_{k-1}^{(i)})$ . According to the state model (15), we partition the components of  $\mathbf{x}_k$  as  $\mathbf{x}_k = [\boldsymbol{\rho}_k^T, \mathbf{s}_k^T]^T$ , where  $\boldsymbol{\rho}_k$  includes the target position and velocity and  $\mathbf{s}_k$  includes the target scattering parameters. Then, we derive a Gibbs sampling algorithm to draw samples  $\mathbf{x}_k^{(i)} \sim p(\mathbf{x}_k|\mathbf{x}_{k-1}^{(i)})$  at the  $k$ th time step in a particle filter. Such a Gibbs sampling is described as follows.

- Initialization,  $j = 0$ . Set randomly or deterministically:

$$\mathbf{x}_k^{(i,0)} = \left[ \left( \boldsymbol{\rho}_k^{(i,0)} \right)^T, \left( \mathbf{s}_k^{(i,0)} \right)^T \right]^T.$$

- Iteration  $j$ ,  $j = 1, \dots, M$ , where  $M$  is a large number.
  - Sample  $\boldsymbol{\rho}_k^{(i,j)} \sim p(\boldsymbol{\rho}_k|\mathbf{s}_k^{(i,j-1)}, \mathbf{x}_{k-1}^{(i)})$ .
  - Sample  $\mathbf{s}_k^{(i,j)} \sim p(\mathbf{s}_k|\boldsymbol{\rho}_k^{(i,j)}, \mathbf{x}_{k-1}^{(i)})$ .
- Installation of  $\boldsymbol{\rho}_k^{(i,M)}$  and  $\mathbf{s}_k^{(i,M)}$  into  $\mathbf{x}_k^{(i)}$ :

$$\mathbf{x}_k^{(i)} = \left[ \left( \boldsymbol{\rho}_k^{(i,M)} \right)^T, \left( \mathbf{s}_k^{(i,M)} \right)^T \right]^T.$$

Then, the obtained  $\mathbf{x}_k^{(i)}$  is a sample from  $p(\mathbf{x}_k|\mathbf{x}_{k-1}^{(i)})$ .

In a special case where the partitions  $\boldsymbol{\rho}$  and  $\mathbf{s}$  are statistical independent of each other, the Gibbs sampling can be simplified as

- Sample  $\boldsymbol{\rho}_k^{(i)} \sim p(\boldsymbol{\rho}_k|\boldsymbol{\rho}_{k-1}^{(i)})$ .
- Sample  $\mathbf{s}_k^{(i)} \sim p(\mathbf{s}_k|\mathbf{s}_{k-1}^{(i)})$ .

Then, we obtain  $\mathbf{x}_k^{(i)} = [(\boldsymbol{\rho}_k^{(i)})^T, (\mathbf{s}_k^{(i)})^T]^T$ .

#### C. Discussion

In the above proposed Gibbs sampling-based particle filter, we use the simplest importance density function  $p(\mathbf{x}_k|\mathbf{x}_{k-1}^{(i)})$ . However, this importance function does not take into account the current measurements  $\mathbf{y}_k$ , and the state space is explored without any knowledge of the observations. Therefore, the filter can be inefficient and it is sensitive to outliers. A natural strategy to overcome this disadvantage is to use an optimal importance function that minimizes the variance of the importance weights conditional upon the states  $\mathbf{x}_{0:k-1}^{(i)}$  and the measurements  $\mathbf{y}_{1:k}$ . Such an optimal importance function is given as [35]

$$q(\mathbf{x}_k|\mathbf{x}_{k-1}^{(i)}, \mathbf{y}_k) = p(\mathbf{x}_k|\mathbf{x}_{k-1}^{(i)}, \mathbf{y}_k) \quad (41)$$

and the importance weight in (39) becomes

$$w_k^{(i)} \propto w_{k-1}^{(i)} p(\mathbf{y}_k|\mathbf{x}_{k-1}^{(i)}). \quad (42)$$

However, this optimal importance function suffers from two drawbacks: it requires the ability to sample from  $p(\mathbf{x}_k|\mathbf{x}_{k-1}^{(i)}, \mathbf{y}_k)$ , which is not easy; and it requires the evaluation of  $p(\mathbf{y}_k|\mathbf{x}_{k-1}^{(i)}) = \int p(\mathbf{y}_k|\mathbf{x}_k)p(\mathbf{x}_k|\mathbf{x}_{k-1}^{(i)})d\mathbf{x}_k$ . This integral has no analytical form in general cases. A practical method to overcome this drawback is to use a Gaussian density to approximate the optimal importance function, which allows us to easily draw samples. The parameters of this Gaussian importance function are evaluated using a local linearization of the original optimal importance function [35], [36]. This method can be extended to use a sum of Gaussian densities to approximate the optimal importance function, which can provide a more accurate approximation when the optimal importance function is multi-modal.

## V. OPTIMAL WAVEFORM DESIGN BASED ON POSTERIOR CRAMÉR-RAO BOUNDS

In this section we propose a new optimal waveform design method for target tracking. This method is based on the proposed dynamic state model and the statistical measurement model in (15) and (26), respectively. It is combined with the above target-tracking algorithms and forms an adaptive waveform design scheme.

In order to pursue the optimization at the  $k$ th time step, we develop an algorithm that predicts the tracking performance at the  $(k+1)$ th time step when employing specific waveform parameters. Then, we select the waveform parameters that optimize a certain criterion. Since the target tracking methods are derived under a sequential Bayesian inference framework, we design the waveform selection criterion based on a posterior Cramér-Rao bound.

### A. Posterior Cramér-Rao Bounds

For random parameters, as in our sequential Bayesian filter for target tracking, a lower bound that is analogous to the Cramér-Rao bound (CRB) in a nonrandom parameter estimation exists and is derived in [37] and [38]. This lower bound is usually referred to as a posterior CRB (PCRB) or a Bayesian CRB.

We denote by  $\mathbf{y}$  a vector of measurements and by  $\mathbf{x}$  a vector of random parameters to be estimated. Let  $p(\mathbf{y}, \mathbf{x})$  be the joint pdf of the pair  $(\mathbf{y}, \mathbf{x})$ , and  $\hat{\mathbf{x}} = \mathbf{g}(\mathbf{y})$  be an estimate of  $\mathbf{x}$ . Then, the PCRB on the mean-square estimation error satisfies

$$\Sigma = \mathbb{E}_{\mathbf{y}, \mathbf{x}} \left[ (\mathbf{g}(\mathbf{y}) - \mathbf{x})(\mathbf{g}(\mathbf{y}) - \mathbf{x})^T \right] \geq J^{-1} \quad (43)$$

where  $J$  is the Bayesian information matrix (BIM),  $J^{-1}$  is the PCRB,  $\mathbb{E}_{\mathbf{y}, \mathbf{x}}[\cdot]$  denotes expectation with respect to  $p(\mathbf{y}, \mathbf{x})$ , and the inequality in the equation means that the difference  $\Sigma - J^{-1}$  is a nonnegative definite matrix. Let  $\Delta_{\psi}^{\eta}$  be the  $m \times n$  matrix of second-order partial derivatives with respect to the  $m$ -dimensional parameter  $\psi$  and  $n$ -dimensional parameter vector  $\eta$ ; i.e.,

$$\Delta_{\psi}^{\eta} = \begin{bmatrix} \frac{\partial^2}{\partial \psi_1 \partial \eta_1} & \cdots & \frac{\partial^2}{\partial \psi_1 \partial \eta_n} \\ \vdots & \ddots & \vdots \\ \frac{\partial^2}{\partial \psi_m \partial \eta_1} & \cdots & \frac{\partial^2}{\partial \psi_m \partial \eta_n} \end{bmatrix}. \quad (44)$$

Using this notation, the BIM for  $\mathbf{x}$  is defined as [38]

$$J = \mathbb{E}_{\mathbf{y}, \mathbf{x}} \left[ -\Delta_{\psi}^{\eta} \log p(\mathbf{y}, \mathbf{x}) \right]. \quad (45)$$

From this property we observe that the PCRB is a lower bound on the error covariance matrix  $\Sigma$ , and it is related only to the state and measurement models and independent of the specific estimation methods. Hence, we can use the PCRB as a precise measure of the tracking system performance.

### B. Criterion for Optimal Waveform Selection

Consider our target tracking problem: at the  $k$ th time step, we want to estimate the state  $\mathbf{x}_k$  using the measurements  $\mathbf{y}_{1:k}$ . We denote by  $\mathbf{X}_k = [\mathbf{x}_0^T, \dots, \mathbf{x}_k^T]^T$  the sequence of states up to time  $k$ . Then, the BIM of the target states, whose inverse is the PCRB, is defined as

$$\bar{J}_k \triangleq \mathbb{E}_{\mathbf{y}_{1:k}, \mathbf{x}_{0:k}} \left[ -\Delta_{\mathbf{X}_k}^{\mathbf{X}_k} \log p(\mathbf{y}_{1:k}, \mathbf{x}_{0:k}) \right]. \quad (46)$$

This BIM and the corresponding PCRB  $\bar{J}_k^{-1}$  are  $(k+1)n_x \times (k+1)n_x$  matrices. The lower right  $n_x \times n_x$  block of  $\bar{J}_k^{-1}$  is the PCRB for estimating  $\mathbf{x}_k$ , and its inverse is the BIM for estimating  $\mathbf{x}_k$ , denoted by  $J_k$ . According to this definition, in our optimal waveform selection algorithm, at the  $k$ th time step we design a criterion based on the BIM  $J_{k+1}$  to select the waveform to be transmitted at the  $(k+1)$ th time step.

To derive the optimal waveform selection criterion, we adopt the recursive equation in [38] to update BIM  $J_{k+1}$ . For the particular case of a linear state model with additive Gaussian noise, this recursive BIM can be written as (see [39])

$$J_{k+1}(\boldsymbol{\theta}_{k+1}) = [Q + FJ_k(\boldsymbol{\theta}_k)^{-1}F^T]^{-1} + \Gamma_{k+1}(\boldsymbol{\theta}_{k+1}) \quad (47)$$

where  $\boldsymbol{\theta}_k$  and  $\boldsymbol{\theta}_{k+1}$  are the waveform parameters at time step  $k$  and  $k+1$ , respectively, and

$$\Gamma_{k+1}(\boldsymbol{\theta}_{k+1}) = \mathbb{E}_{\mathbf{y}_{k+1}, \mathbf{x}_{k+1}} \left[ -\Delta_{\mathbf{x}_{k+1}}^{\mathbf{x}_{k+1}} \log p(\mathbf{y}_{k+1}(\boldsymbol{\theta}_{k+1})|\mathbf{x}_{k+1}) \right]. \quad (48)$$

In our sequential waveform design algorithm, we attempt to minimize the error on the estimation of the target state using the information provided by the state and measurement models and the measurement history  $\mathbf{y}_{1:k}$ . Hence, we modify the matrix  $\Gamma_{k+1}$  to include the measurement history and design a criterion based on a new matrix  $\tilde{\Gamma}_{k+1}$ :

$$\tilde{\Gamma}_{k+1}(\boldsymbol{\theta}_{k+1}) = \mathbb{E}_{\mathbf{y}_{k+1}, \mathbf{x}_{k+1}|\mathbf{y}_{1:k}} \left[ -\Delta_{\mathbf{x}_{k+1}}^{\mathbf{x}_{k+1}} \log p(\mathbf{y}_{k+1}(\boldsymbol{\theta}_{k+1})|\mathbf{x}_{k+1}) \right]. \quad (49)$$

By replacing  $\Gamma_{k+1}$  with  $\tilde{\Gamma}_{k+1}$ , we use the information from the measurement history  $\mathbf{y}_{1:k}$  to improve our prior knowledge on the state  $\mathbf{x}_{k+1}$ . Mathematically, we replace the prior density  $p(\mathbf{x}_{k+1})$  with  $p(\mathbf{x}_{k+1}|\mathbf{y}_{1:k})$  when calculating  $\Gamma_{k+1}$  (see (52) for a further understanding). Hence,  $\tilde{\Gamma}_{k+1}$  provides more information on state  $\mathbf{x}_{k+1}$  than  $\Gamma_{k+1}$ , and the waveform selection criterion based on  $\tilde{\Gamma}_{k+1}$  has the potential to provide better processing performance. Note that  $\tilde{\Gamma}_{k+1}$  is calculated by averaging over all the possible values of  $\mathbf{y}_{k+1}$ . That means we do not need to know



the specific value of the next measurements to calculate the criterion function. Then, for selecting the optimal parameters of the next transmitted waveform, we propose to use the weighted trace of the inverse of (47), replacing  $\Gamma_{k+1}$  by  $\tilde{\Gamma}_{k+1}$

$$\boldsymbol{\theta}_{k+1}^* = \arg \min_{\boldsymbol{\theta}_{k+1} \in \Theta} \text{Tr} \left\{ \Pi \tilde{\Gamma}_{k+1}^{-1}(\boldsymbol{\theta}_{k+1}) \right\} \quad (50)$$

where  $\Theta$  denotes a set of the allowed values for  $\boldsymbol{\theta}_{k+1}$  or a library of all possible waveforms,  $\Pi$  is the weighting matrix used to equalize the magnitude of the different parameters in the state vector (see also [7]), and  $\tilde{\Gamma}_{k+1}$  is defined as in (47) replacing  $\Gamma_{k+1}$  by  $\tilde{\Gamma}_{k+1}$ .

### C. Computation of the Criterion Function

The proposed criterion function depends not only on the information provided by the state model  $F$  but also on the measurement model and history, through the term  $\tilde{\Gamma}_{k+1}$ . To compute the former matrix, in general, the expectation in (49) has no closed-form analytical solution and must be solved numerically. We propose to use Monte Carlo integration to calculate this expectation and merge this numerical procedure into the sequential Monte Carlo method for tracking the target.

In order to compute the numerical result for  $\tilde{\Gamma}_{k+1}$ , we define the matrix function

$$\Lambda(\mathbf{y}_{k+1}, \mathbf{x}_{k+1}) = -\Delta_{\mathbf{x}_{k+1}}^{\mathbf{x}_{k+1}} \log p(\mathbf{y}_{k+1} | \mathbf{x}_{k+1}). \quad (51)$$

Then, we can rewrite  $\tilde{\Gamma}_{k+1}$  as

$$\tilde{\Gamma}_{k+1} = \int_{\mathbf{x}_{k+1}} \left[ \int_{\mathbf{y}_{k+1}} \Lambda(\mathbf{y}_{k+1}, \mathbf{x}_{k+1}) p(\mathbf{y}_{k+1} | \mathbf{x}_{k+1}) d\mathbf{y}_{k+1} \right] \times p(\mathbf{x}_{k+1} | \mathbf{y}_{1:k}) d\mathbf{x}_{k+1}. \quad (52)$$

According to this equation, the expectation to calculate  $\tilde{\Gamma}_{k+1}$  can first be taken with respect to the conditional density function  $p(\mathbf{y}_{k+1} | \mathbf{x}_{k+1})$  and then with respect to the density  $p(\mathbf{x}_{k+1} | \mathbf{y}_{1:k})$ ; i.e.,

$$\tilde{\Gamma}_{k+1} = \mathbb{E}_{\mathbf{x}_{k+1} | \mathbf{y}_{1:k}} [\Xi_{k+1}] \quad (53)$$

$$\Xi_{k+1} = \mathbb{E}_{\mathbf{y}_{k+1} | \mathbf{x}_{k+1}} [-\Delta_{\mathbf{x}_{k+1}}^{\mathbf{x}_{k+1}} \log p(\mathbf{y}_{k+1} | \mathbf{x}_{k+1})]. \quad (54)$$

Note that  $\Xi_{k+1}$  is the standard Fisher information matrix (FIM) for estimating the state vector  $\mathbf{x}_{k+1}$  based on the observations  $\mathbf{y}_{k+1}$ .

In order to calculate (53), we need samples of the predicted target state  $\mathbf{x}_{k+1}$ . We can apply sequential Monte Carlo methods to draw these samples. For a sequential Monte Carlo method, we obtain  $N_s$  samples and its associated weights at the  $k$ th time step from the belief  $p(\mathbf{x}_k | \mathbf{y}_{1:k})$  as  $\{\mathbf{x}_k^{(i)}, w_k^{(i)}; i = 1, \dots, N_s\}$ . Then, the corresponding samples and weights of the predicted state are  $\{\mathbf{x}_{k+1}^{(i)}, w_k^{(i)}; i = 1, \dots, N_s\}$ , where  $\mathbf{x}_{k+1}^{(i)} \sim p(\mathbf{x}_{k+1} | \mathbf{x}_k^{(i)})$  (see Appendix A for details). Therefore, the expectation in (53) can be computed by the following two steps:

- For  $i = 1, \dots, N_s$ , draw samples  $\mathbf{x}_{k+1}^{(i)} \sim p(\mathbf{x}_{k+1} | \mathbf{x}_k^{(i)})$ .

- Approximate the matrix  $\tilde{\Gamma}_{k+1}$  as

$$\tilde{\Gamma}_{k+1} \approx \sum_{i=1}^{N_s} w_k^{(i)} \Xi_{k+1}(\mathbf{x}_{k+1}^{(i)}). \quad (55)$$

In order to calculate (54), for each  $\mathbf{x}_{k+1}^{(i)}$ , we draw  $N_y$  identically independently distributed (i.i.d.) samples  $\{\mathbf{y}_{k+1}^{(j)}; j = 1, \dots, N_y\}$  from the likelihood function  $p(\mathbf{y}_{k+1} | \mathbf{x}_{k+1}^{(i)})$ . Then, we approximate the FIM  $\Xi_{k+1}(\mathbf{x}_{k+1}^{(i)})$  as

$$\Xi_{k+1}(\mathbf{x}_{k+1}^{(i)}) \approx \frac{1}{N_y} \sum_{j=1}^{N_y} \Lambda(\mathbf{y}_{k+1}^{(j)}, \mathbf{x}_{k+1}^{(i)}). \quad (56)$$

Therefore, we approximate  $\tilde{\Gamma}_{k+1}$  using the Monte Carlo method as

$$\tilde{\Gamma}_{k+1} \approx \frac{1}{N_y} \sum_{i=1}^{N_s} \sum_{j=1}^{N_y} w_k^{(i)} \Lambda(\mathbf{y}_{k+1}^{(j)}, \mathbf{x}_{k+1}^{(i)}). \quad (57)$$

1) *Computation under Gaussian Measurement Noise:* The Monte Carlo integration for computing  $\tilde{\Gamma}_{k+1}$  given by (57) is suitable for any statistical measurement model. However, if the additive noise  $\mathbf{e}_k$  in the measurement model (26) has Gaussian distribution, we can obtain an analytical form for the FIM  $\Xi_{k+1}$ ; thus, the cost of computing  $\tilde{\Gamma}_{k+1}$  using (53) can be significantly reduced.

Assuming that the measurement noise  $\mathbf{e}_{k+1}$  follows a complex Gaussian distribution, the measurement  $\mathbf{y}_{k+1}$  given  $\mathbf{x}_{k+1}$  is distributed as

$$\mathbf{y}_{k+1} | \mathbf{x}_{k+1} \sim \mathcal{CN}(\mathbf{h}(\mathbf{x}_{k+1}), \Sigma_{k+1}) \quad (58)$$

where  $\mathbf{h}(\cdot)$  is defined in (26). We also assume that the measurement noise values  $\{\mathbf{e}_{k+1}(t), t = t_1, \dots, t_N\}$  are independent at different sample times. Then, the covariance matrix in (58) can be written as a block diagonal matrix:

$$\Sigma_{k+1} = \text{diag} \{ \Sigma_{k+1}(t_1), \dots, \Sigma_{k+1}(t_N) \} \quad (59)$$

where, if the measurement noise  $\mathbf{e}_{k+1}$  follows the model described in Section III-B-2,

$$\Sigma_{k+1}(t) = A(\phi_0, \psi_0) \xi(t - \tau_0) \Sigma_c \xi^H(t - \tau_0) A^H(\phi_0, \psi_0) + \sigma^2 I_{6M}. \quad (60)$$

Therefore, according to the results in [40, Ch. 15.7] the FIM in (54) is

$$[\Xi_{k+1}(\mathbf{x}_{k+1})]_{ij} = 2 \sum_{t=t_1}^{t_N} \text{Re} \left\{ \left[ \frac{\partial \tilde{\mathbf{h}}(t, \mathbf{x}_{k+1})}{\partial x_{k+1,i}} \right]^H \Sigma_{k+1}^{-1}(t) \times \left[ \frac{\partial \tilde{\mathbf{h}}(t, \mathbf{x}_{k+1})}{\partial x_{k+1,j}} \right] \right\} \quad (61)$$

where  $\tilde{\mathbf{h}}(\cdot)$  is defined in (25).

2) *Suboptimal Criterion Function:* Computing  $\tilde{\Gamma}_{k+1}$  using the Monte Carlo integration is intensive and time demanding because the FIM  $\Xi_{k+1}$  must be evaluated for every particle. Therefore, we propose a suboptimal criterion function in which

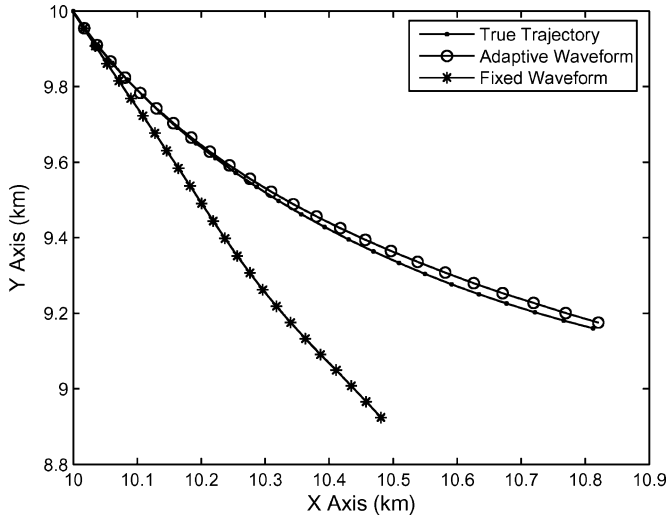


Fig. 1. Comparison of the averaged tracking results between adaptive and fixed waveform schemes.

the matrix  $\tilde{\Gamma}_{k+1}$  is replaced by  $\Xi_{k+1}$  evaluated at the expected predicted state. Therefore, the suboptimal criterion can be computed by the following steps:

- For  $i = 1, \dots, N_s$ , draw samples  $\mathbf{x}_{k+1}^{(i)} \sim p(\mathbf{x}_{k+1} | \mathbf{x}_k^{(i)})$ .
- The expectation of the predicted state is approximated as

$$\hat{\mathbf{x}}_{k+1} \approx \sum_{i=1}^{N_s} w_k^{(i)} \mathbf{x}_{k+1}^{(i)}. \quad (62)$$

- Replace  $\tilde{\Gamma}_{k+1}$  by  $\Xi_{k+1}(\hat{\mathbf{x}}_{k+1})$  in (47).

This suboptimal criterion significantly reduces computation time at the expense of accuracy in computing the integral; hence, the selected waveform may not be optimal.

## VI. NUMERICAL EXAMPLES

In this section, we use numerical examples to study the performance of the proposed adaptive waveform design method for tracking targets in the presence of clutter. Through these examples we demonstrate the advantages of the adaptive waveform design scheme compared with the fixed transmitted waveform scheme. We also study how the target scattering coefficients will affect the design of the polarimetric aspect of the waveform. First, we provide a description of the simulation setup considered for the target and tracking system, and then we discuss different numerical examples. The results reported in this section correspond to the average over 100 Monte Carlo simulations.

*Target and Clutter:* The numerical examples consist of a single target that moves parallel to the horizontal plane at a velocity of 200 m/s. The target trajectory is a section of a circle of radius 1.5 km, that starts at the position  $\mathbf{r}_0 = [10, 10]$  km, as shown in Fig. 1. We assume that the scattering parameters of the target are partially known and have the following values:  $m = 1$ ,  $\epsilon = 15^\circ$ ,  $\rho = 0^\circ$ ,  $\nu = 0^\circ$ , and  $\gamma = 20^\circ$ ; however, its orientation angle  $\vartheta$  can change as the target moves. In addition, we consider that the clutter covariance parameters have been estimated using training data and that they have the following values:  $\vartheta_c = 85^\circ$ ,  $\epsilon_c = 5^\circ$ ,  $\sigma_p^2 = 0.4$ ,  $\sigma_u^2 = 0.4$ , and  $p_x = 0.2$ .

The covariance of the clutter will be scaled to fulfill the required target-to-clutter ratio (TCR). The definition of TCR is given in Appendix B.

*Transmitted Signal:* We consider a radar system that transmits one pulse ( $L = 1$ ) at intervals of  $T_{\text{PRI}} = 250$  ms, with a carrier frequency  $f_c = 15$  GHz ( $\lambda = 20$  mm). The maximum signal bandwidth is  $BW_{\text{max}} = 500$  kHz. The system is capable of transmitting LFM pulses that change length  $\eta$ , frequency rate  $b$ , and polarization angles  $\alpha$  and  $\beta$  on a pulse-to-pulse basis.

*Tracking System:* The receiver of the tracker consists of two vector sensors ( $M = 2$ ) located at  $\mathbf{r}_1 = [-0.25\lambda, 0]$  and  $\mathbf{r}_2 = [0.25\lambda, 0]$ . The radar echoes are recorded at sampling frequency  $f_s = 1$  MHz. The system tracks the position and velocity of the target, as well as its orientation angle; hence, the state vector is  $\mathbf{x} = [x, \dot{x}, y, \dot{y}, \vartheta]^T$ . The particle filter is implemented using the transitional prior  $p(\mathbf{x}_k | \mathbf{x}_{k-1}^{(i)})$  as the importance density function to draw  $N_s = 500$  particles. The intensity of the process noise is given by  $q_p = 500$  and  $q_s = 50$ . In addition, we assume the covariance of the initial state is  $J_0^{-1} = \text{diag}[500, 500, 200, 200, 0.5]$ . The weighting matrix  $\Pi$  is a diagonal matrix whose main diagonal entries are a power of ten intended to equalize the covariance of the different parameters.

*Example 1:* In this example, we compare the performance of the adaptive and fixed waveform system assuming that the orientation angle of the target is  $\vartheta = 0^\circ$  along the entire trajectory. For the adaptive system, the wave shape parameters are  $\eta = 100 \mu\text{s}$  and  $b_{\text{max}} = BW_{\text{max}}/7.4\eta$  (maximum allowable frequency rate for the signal bandwidth), and the polarization aspects of the signal are selected from the following waveform library:

$$\Theta = \{\boldsymbol{\theta}_{ln} = (\alpha_l, \beta_n, \eta, b); l = 0, \dots, 36; n = 0, \dots, 6\} \quad (63)$$

where

$$\alpha_l = -90^\circ + l \cdot 5^\circ, \quad \beta_n = -45^\circ + n \cdot 15^\circ. \quad (64)$$

For the fixed waveform, the transmitted signal corresponds to the waveform  $\boldsymbol{\theta}_{0,3}$  (vertical polarization). Fig. 1 shows the averaged tracking results of the moving target in an environment such that  $\text{TCR} = 10$  dB and [signal-to-noise ratio (SNR)]  $\text{SNR} = 10$  dB. For the fixed waveform, the vertical polarization is unfavorable because it is close to the polarimetric response of the clutter. Hence, the received signal is highly corrupted by clutter reflections and the tracking filter is not capable of following the target. On the other hand, the adaptive waveform method, although it was also started with vertical polarization, immediately selects the waveform that matches the target polarimetric aspects, increasing the energy of the signal reflected from the target and reducing the clutter reflections. Therefore, the tracking performance for the adaptive waveform selection scheme is significantly better than the fixed waveform scheme.

Using the same simulation setup, the numerical example was repeated. However, this time the waveform was selected by applying the suboptimal criterion function in order to reduce the computation cost of the adaptive waveform design algorithm. Fig. 2 shows the square root of the averaged MSE for the target position. As expected, the suboptimal algorithm generated estimates with larger error. However, since the loss of performance

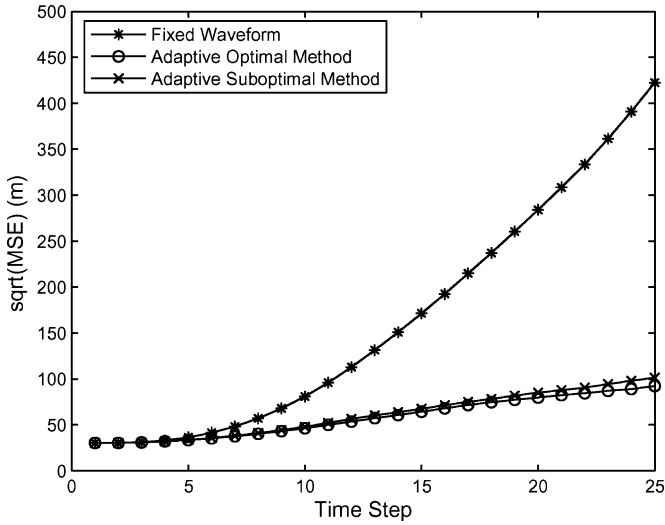


Fig. 2. Square root of the averaged MSE for the target position.

is small and the reduction of computation time is significant, we will apply this suboptimal method in the following examples.

*Example 2:* In this new example, we study the performance of the adaptive system when the transmit signal is also allowed to have different shape parameters. In this case, the waveform library consists of  $\Theta = \{\theta_{lrs} = (\alpha_l, \beta_n, \eta_r, b_s); l = 0, \dots, 36; n = 0, \dots, 6; r = 0, \dots, 9; s = 0, \dots, 2\}$  (65)

where  $\alpha_l = -90^\circ + l \cdot 5^\circ$ ,  $\beta_n = -45^\circ + n \cdot 15^\circ$   
 $\eta_r = 10 \mu\text{s} + r \cdot 10 \mu\text{s}$ ,  $b_s \in \{-b_{max}, 0, b_{max}\}$  (66)

where  $b_{max}$  is the maximum frequency rate for a given  $\eta$ .

The simulations show that our adaptive waveform algorithm always selects the waveforms with the longest length and highest frequency rate; i.e.  $\eta = 100 \mu\text{s}$  and  $b = b_{max}$ . We note that longer pulses reduce the estimation error for the target velocity and signals with higher frequency rate reduce the error on the position. Hence, in order to estimate both position and velocity of the target, the adaptive waveform algorithm selects the signal with the largest length and frequency rate. Note that signals with highest time-bandwidth product are frequently applied in radar.

The waveform selection algorithm selects the polarization parameters of the signal in order to increase the energy of the target echoes and to reduce the energy from the clutter, as was discussed in the previous example.

*Example 3:* We analyze the behavior of the tracking filter when the state model does not match the target dynamics. In this case, we consider the setup and waveform library as in the first example; however, the orientation angle of the target  $\vartheta$  changes following the linear piecewise function depicted in Fig. 3. The same figure shows the estimated target orientation angle and the waveform polarization angle  $\alpha$  selected for transmission by the adaptive algorithm. The same simulation was solved for two scenarios:  $\text{TCR} = \text{SNR} = 10 \text{ dB}$  and  $\text{TCR} = \text{SNR} = 15 \text{ dB}$ .

In Fig. 3, it can be observed that the filter tries to track the true orientation angle when it is changing linearly, even though this parameter is defined as constant in the state model. Clearly,

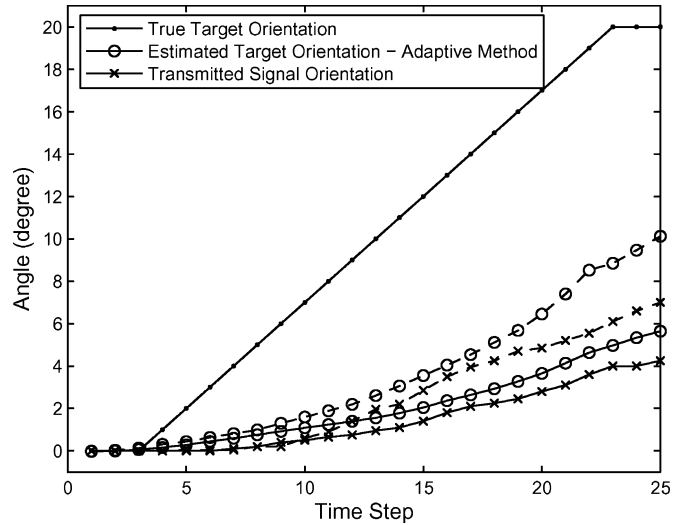


Fig. 3. Averaged orientation angles for two scenarios:  $\text{TCR} = \text{SNR} = 10 \text{ dB}$  (solid line) and  $\text{TCR} = \text{SNR} = 15 \text{ dB}$  (dotted line).

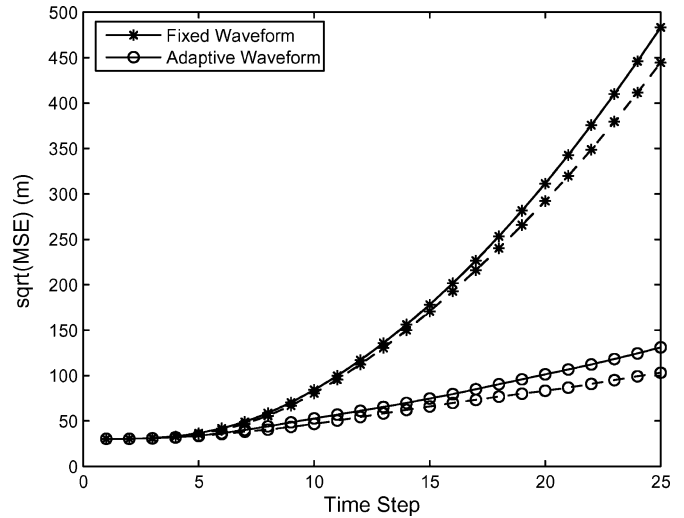


Fig. 4. Square root of the averaged MSE for the target position for two scenarios:  $\text{TCR} = \text{SNR} = 10 \text{ dB}$  (solid line) and  $\text{TCR} = \text{SNR} = 15 \text{ dB}$  (dotted line).

the convergence of the estimated orientation angle is faster when the clutter and noise interference is lower. We note that the filter selects the waveform that best matches the estimated target polarization aspects, in order to increase the energy reflected by the target.

In addition, we studied the performance of the adaptive method with respect to the fixed waveform system. Fig. 4 and Fig. 5 depict the square root of the averaged MSE for the target position and orientation angle, respectively. It is not surprising that estimation performance is better in the case of lower clutter and noise interference for both the fixed and adaptive case. It is also interesting to note that the estimation performance on the position for the adaptive case is worse with respect to Example 1. The reason for this lower performance is because the target orientation is changing and the tracking filter cannot estimate precisely that target parameter. In such a case, the adaptive waveform algorithm selects the signal that matches the

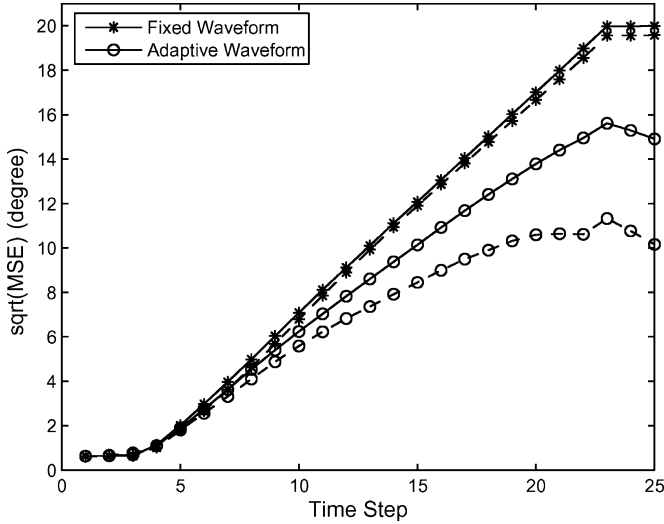


Fig. 5. Square root of the averaged MSE for the target orientation angle for two scenarios: TCR = SNR = 10 dB (solid line) and TCR = SNR = 15 dB (dotted line).

estimated target parameters, which differs from the true target parameters. Nevertheless, the adaptive system still performs better than the fixed waveform system for this example.

## VII. CONCLUSIONS

In this paper, we addressed the problem of adaptive polarized waveform design for tracking a target in the presence of clutter. We proposed a general framework based on sequential Bayesian inference. For the target-tracking problem, we adopted a sequential Monte Carlo method that is very powerful for handling nonlinear and non-Gaussian state and measurement models. We first defined a state model that includes the scattering coefficients of the target in addition to its position and velocity. We proposed and developed a measurement model that is the output of an EM vector-sensor array. This model provides a natural way of introducing polarimetric information of both target and clutter into the tracking filter. Then, we developed an adaptive waveform design scheme that exploits the freedom provided by the polarization of the transmitted waveform to increase tracking accuracy. We derived a new criterion based on a posterior Cramér-Rao bound to optimally select the waveform one step ahead on time. We also applied a Monte Carlo method to compute this criterion numerically and proposed a suboptimal method that considerably reduces the computation cost. Numerical examples demonstrated the advantages of the adaptive waveform design scheme. Specifically, we showed that selecting the optimal signal polarization improves the tracker performance.

In future work, we will validate our algorithms using real radar data. In addition, we will apply the proposed framework for adaptive waveform design to other radar applications, e.g., target sequential detection. We will derive more realistic dynamic state models to track the target scattering coefficients and other target states. We will also incorporate other clutter

models into the statistical measurement model according to different application scenarios. Our proposed framework for adaptive waveform design provides us the freedom to implement different criteria to optimally select the next transmitted waveform parameters. Hence, in our future work, we will implement and compare different waveform design criteria for different applications and operational scenarios.

## APPENDIX

### A. Numerical Computation of (53)

In order to compute the expectation in (53) using Monte Carlo integration, we need to draw samples from certain importance density function and find their corresponding importance weights. We start by finding an approximation to the prediction of the belief

$$p(\mathbf{x}_{0:k+1}|\mathbf{y}_{1:k}) \approx \sum_{i=1}^{N_s} \varpi_{k+1}^{(i)} \delta(\mathbf{x}_{0:k+1} - \mathbf{x}_{0:k+1}^{(i)}). \quad (\text{A.1})$$

As in the procedure described in Section IV-A, the weights  $\varpi_{k+1}^{(i)}$  are chosen using the principle of importance sampling:

$$\varpi_{k+1}^{(i)} \propto \frac{p(\mathbf{x}_{0:k+1}^{(i)}|\mathbf{y}_{1:k})}{g(\mathbf{x}_{0:k+1}^{(i)}|\mathbf{y}_{1:k})} \quad (\text{A.2})$$

where  $g(\cdot)$  is the importance density function to be specified. Considering that this function should also satisfy the assumptions A1 and A2, then it can be factored as

$$g(\mathbf{x}_{0:k+1}|\mathbf{y}_{1:k}) = g(\mathbf{x}_{k+1}|\mathbf{x}_k)g(\mathbf{x}_{0:k}|\mathbf{y}_{1:k}). \quad (\text{A.3})$$

Applying the same decomposition to the prediction of the belief, the weights are

$$\varpi_{k+1}^{(i)} \propto \frac{p(\mathbf{x}_{0:k}|\mathbf{y}_{1:k})p(\mathbf{x}_{k+1}|\mathbf{x}_k)}{g(\mathbf{x}_{0:k}|\mathbf{y}_{1:k})g(\mathbf{x}_{k+1}|\mathbf{x}_k)}. \quad (\text{A.4})$$

If the importance density function  $g$  is chosen to match importance density function  $q$  of the tracking particle filter, the weights become (see (38))

$$\varpi_{k+1}^{(i)} \propto w_k^{(i)} \frac{p(\mathbf{x}_{k+1}|\mathbf{x}_k)}{q(\mathbf{x}_{k+1}|\mathbf{x}_k)}. \quad (\text{A.5})$$

Furthermore, if the importance density  $q$  of the tracking particle filter is the prior  $p(\mathbf{x}_{k+1}|\mathbf{x}_k)$ , the weights of the filter and the numerical integral are equal. Hence, the prediction of the belief can be approximated as

$$p(\mathbf{x}_{k+1}|\mathbf{y}_{1:k}) \approx \sum_{i=1}^{N_s} w_k^{(i)} \delta(\mathbf{x}_{k+1} - \mathbf{x}_{k+1}^{(i)}). \quad (\text{A.6})$$

Finally, (53) can be computed as in (55).

### B. Definition of TCR and SNR

In order to characterize the target in its environment, we define the TCR following the work by Novak *et al.* in [41]

$$\text{TCR} = \frac{\| [s_{\text{hh}}, s_{\text{vv}}, s_{\text{hv}}] \|^2}{\text{tr}(\Sigma_C)} \quad (\text{B.1})$$

where  $s_{hh}$ ,  $s_{vv}$ ,  $s_{hv}$  are the target scattering coefficients defined in (10) and  $\|\cdot\|$  is the norm of the vector.

When selecting the optimal signal parameters, the pulse length and bandwidth of the signal are changed. Hence, we seek to specify a definition of the SNR independent of these features. Then, it is useful to define SNR as

$$\text{SNR} = \frac{\int_{t_i}^{t_f} |p(t)|^2 \partial t}{\int_{t_i}^{t_f} \text{E} \left[ |n(t)|^2 \right] \partial t} = \frac{L}{\sigma^2(t_f - t_i)} \quad (\text{B.2})$$

where  $L$  is the number of transmitted pulses,  $\sigma^2$  is the power of the thermal noise process and  $t_i$ ,  $t_f$  define the time-window during which the system is allowed to track the target. For the simulation examples, these parameters were set up in a way that the system was able to follow a target in a radial distance between 10 and 25 km.

## REFERENCES

- [1] M. Bell, "Information theory and radar waveform design," *IEEE Trans. Inf. Theory*, vol. 39, no. 5, pp. 1578–1597, Sep. 1993.
- [2] S. M. Sowelam and A. H. Tewfik, "Waveform selection in radar target classification," *IEEE Trans. Inf. Theory*, vol. 46, no. 3, pp. 1014–1029, May 2000.
- [3] D. G. Giuli, "Polarization diversity in radars," *Proc. IEEE*, vol. 74, pp. 245–269, Feb. 1986.
- [4] A. Nehorai and E. Paldi, "Vector-sensor array processing for electromagnetic source localization," *IEEE Trans. Signal Process.*, vol. 42, no. 2, pp. 376–398, Feb. 1994.
- [5] B. Hochwald and A. Nehorai, "Polarimetric modeling and parameters estimation with applications to remote sensing," *IEEE Trans. Signal Process.*, vol. 43, no. 8, pp. 1923–1935, Aug. 1995.
- [6] J. Wang and A. Nehorai, "Adaptive polarimetric design for a target in compound-Gaussian clutter," presented at the Int. Waveform Diversity and Design Conf., Special Session on Signal Process. Waveform Diversity and Design, Lihue, HI, Jan. 2006.
- [7] M. Hurtado and A. Nehorai, "Optimal polarized waveform design for active target parameter estimation using electromagnetic vector sensors," in *Proc. IEEE Int. Conf. Acoust., Speech, Signal Process.*, Toulouse, France, May 2006, vol. 5, pp. 1125–1128.
- [8] D. J. Kershaw and R. J. Evans, "Optimal waveform selection for tracking systems," *IEEE Trans. Inf. Theory*, vol. 40, no. 5, pp. 1536–1550, Sep. 1994.
- [9] D. J. Kershaw and R. J. Evans, "Waveform selective probabilistic data association," *IEEE Trans. Aerosp. Electron. Syst.*, vol. 33, no. 4, pp. 1180–1188, Oct. 1997.
- [10] S. Suvorova, D. Musicki, B. Moran, S. D. Howard, and B. La Scala, "Multi step ahead beam and waveform scheduling for tracking of maneuvering targets in clutter," in *Proc. Special Session on Adv. Waveform Agile Sensor Process.*, *IEEE Int. Conf. Acoust., Speech, Signal Process.*, Philadelphia, PA, Mar. 2005, pp. 889–892.
- [11] S. Suvorova and S. D. Howard, "Waveform libraries for radar tracking applications: Maneuvering targets," presented at the Special Session on Waveform Adaptive Sensing, Conf. Inf. Sci. Syst., Princeton, NJ, Mar. 2006.
- [12] S. P. Sira, A. Papandreou-Suppappola, and D. Morrell, "Waveform and scheduling for agile sensors for target tracking," in *Proc. 38th Asilomar Conf. Signal, Syst., Comput.*, Pacific Grove, CA, Nov. 2004, vol. 1, pp. 820–824.
- [13] S. P. Sira, A. Papandreou-Suppappola, and D. Morrell, "Time-varying waveform selection and configuration for agile sensors in tracking applications," in *Proc. IEEE Int. Conf. Acoust., Speech, Signal Process. (ICASSP), Special Session on Advances in Waveform Agile Sensor Process.*, Philadelphia, PA, Mar. 2005, vol. 5, pp. 881–884.
- [14] S. P. Sira, A. Papandreou-Suppappola, and D. Morrell, "Characterization of waveform performance in dynamically configured sensor systems," presented at the Int. Waveform Diversity and Design Conf., Special Session on Signal Process. Waveform Diversity and Design, Lihue, HI, Jan. 2006.
- [15] S. P. Sira, A. Papandreou-Suppappola, D. Morrell, and D. Cochran, "Waveform-agile sensing for tracking multiple targets in clutter," in *Proc. Conf. Inf. Sci. Syst., Special Session on Waveform Adaptive Sensing*, Princeton, NJ, Mar. 2006, pp. 1418–1423.
- [16] S. P. Sira, A. Papandreou-Suppappola, and D. Morrell, "Waveform scheduling in wideband environments," in *Proc. IEEE Int. Conf. Acoust., Speech, Signal Process. (ICASSP), Special Session on Waveform Diverse Sens. Syst.*, Toulouse, France, May 2006, vol. 5, pp. 1121–1124.
- [17] C. M. S. See and A. Nehorai, "Source localization with distributed electromagnetic component sensor array processing," in *Int. Symp. Signal Process. Its Appl.*, Jul. 2003, vol. 1, pp. 231–236.
- [18] M. Hurtado and A. Nehorai, "Performance analysis of passive low-grazing-angle source localization in maritime environments using vector sensors," *IEEE Trans. Aerosp. Electron. Syst.*, to be published.
- [19] R. Compton, "The tripole antenna: An adaptive array with full polarization flexibility," *IEEE Trans. Antennas Propag.*, vol. AP-29, no. 6, pp. 944–952, Nov. 1981.
- [20] E. Ferrara and T. Parks, "Direction finding with an array of antennas having diverse polarizations," *IEEE Trans. Antennas Propag.*, vol. AP-31, no. 2, pp. 231–236, Mar. 1983.
- [21] M. Chu, H. Haussecker, and F. Zhao, "Scalable information-driven sensor querying and routing for ad hoc heterogeneous sensor networks," *Int. J. High-Perform. Comput. Appl.*, vol. 16, no. 3, pp. 90–110, 2002.
- [22] J. R. Huynen, "Measurement of the target scattering matrix," *Proc. IEEE*, vol. 53, pp. 936–946, Aug. 1965.
- [23] V. Karyshev, V. A. Khlusov, L. P. Lighthart, and G. Sharygin, "Algorithms for estimating the complete group of polarization invariants of the scattering matrix (SM) based on measuring all SM elements," *IEEE Trans. Geosci. Remote Sens.*, vol. 42, no. 3, pp. 529–539, Mar. 2004.
- [24] Y. Bar-Shalom, X.-R. Li, and T. Kirubarajan, *Estimation With Applications To Tracking and Navigation*. New York: Wiley, 2001.
- [25] D. J. McLaughlin, N. Allan, E. M. Twarog, and D. B. Trizna, "High resolution polarimetric radar scattering measurements of low grazing angle sea clutter," *IEEE J. Ocean. Eng.*, vol. 20, no. 3, pp. 166–178, Jul. 1995.
- [26] K. D. Ward, C. J. Baker, and S. Watts, "Maritime surveillance radar. Part 1: Radar scattering from the ocean surface," *Inst. Elect. Eng. Proc.*, vol. 137, pp. 51–62, Jul. 1990.
- [27] E. Conte and M. Longo, "Characterisation of radar clutter as a spherically invariant random process," *Inst. Elect. Eng. Proc.-F*, vol. 134, pp. 191–197, Apr. 1997.
- [28] M. Hurtado and A. Nehorai, "Polarimetric detection of targets in inhomogeneous clutter," in *Proc. 15th Annu. Workshop Adaptive Sens. Array Process.*, Lexington, MA, Jun. 5–6, 2007, Lincoln Lab., to be published.
- [29] B. Ristic, S. Arulampalam, and N. Gordon, *Beyond the Kalman Filter—Particle Filters for Tracking Applications*. Dedham, MA: Artech House, 2004.
- [30] C. P. Robert and G. Casella, *Monte Carlo Statistical Methods*. New York: Springer-Verlag, 1999.
- [31] C. Andrieu, A. Doucet, and W. J. Fitzgerald, "An introduction to Monte Carlo methods for Bayesian data analysis," in *Nonlinear Dynamics and Statistics*, A. I. Mees, Ed. Boston, MA: Birkhäuser, 2001.
- [32] B. P. Carlin, N. G. Polson, and D. S. Stoffer, "A Monte Carlo approach to nonnormal and nonlinear state-space modeling," *J. Amer. Statist. Assoc.*, vol. 87, no. 418, Jun. 1992.
- [33] A. Doucet, J. F. G. de Freitas, and N. J. Gordon, "An introduction to sequential Monte Carlo methods," in *Sequential Monte Carlo Methods in Practice*, A. Doucet, J. F. G. de Freitas, and N. J. Gordon, Eds. New York: Springer-Verlag, 2001.
- [34] M. S. Arulampalam, S. Maskell, N. J. Gordon, and T. Clapp, "A tutorial on particle filters for online nonlinear/non-Gaussian Bayesian tracking," *IEEE Trans. Signal Process.*, vol. 50, no. 2, pp. 174–188, Feb. 2002.
- [35] A. Doucet, S. Godsill, and C. Andrieu, "On sequential Monte Carlo sampling methods for Bayesian filtering," *Statist. Comput.*, vol. 10, no. 3, pp. 197–208, 2000.
- [36] M. Orton and W. Fitzgerald, "A Bayesian approach to tracking multiple targets using sensor arrays and particle filters," *IEEE Trans. Signal Process.*, vol. 53, no. 2, pp. 216–223, Feb. 2002.
- [37] H. L. van Trees, *Estimation and Modulation Theory*. New York: Wiley, 1968.
- [38] P. Tichavský, C. H. Muravchik, and A. Nehorai, "Posterior Cramér-Rao bounds for discrete-time nonlinear filtering," *IEEE Trans. Signal Process.*, vol. 46, no. 5, May 1998.

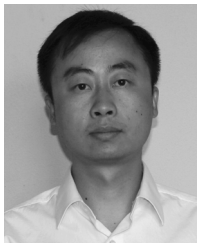
- [39] K. L. Bell and H. L. van Tress, "Posterior Cramér-Rao bound for tracking target bearing," presented at the 13th Annu. Workshop Adaptive Sens. Array Process. (ASAP '05), Lincoln, Lab., Lexington, MA, Jun. 7–8, 2005.
- [40] S. M. Kay, *Fundamentals of Statistical Signal Processing: Estimation Theory*. Englewood Cliffs, NJ: Prentice-Hall, Inc., 1993.
- [41] R. D. Chaney, M. C. Bud, and L. M. Novak, "On the performance of polarimetric target detection algorithms," *IEEE Aerosp. Electron. Syst. Mag.*, vol. 5, no. 11, pp. 10–15, Nov. 1990.



**Martin Hurtado** received the B.Eng. and M.Sc. degrees in electrical engineering from the National University of La Plata, Argentina, in 1996 and 2001, respectively. He received the Ph.D. degree in electrical engineering from Washington University, St. Louis, in 2007, under the guidance of Prof. A. Nehorai.

Currently, he is a Postdoctoral Research Associate with the Department of Electrical and Systems Engineering, Washington University, St. Louis. His research interests are in the area of statistical

signal processing, detection and estimation theory, and their applications in sensor arrays, communications, and remote sensing systems. In addition, he is interested in electromagnetic theory and antenna design.



**Tong Zhao** (S'02–M'07) received the B.Eng. and M.Sc. degrees in electrical engineering from the University of Science and Technology of China (USTC), Hefei, in 1997 and 2000, respectively. He received the Ph.D. degree in electrical engineering from Washington University, Saint Louis, in 2006, under the guidance of Prof. A. Nehorai.

From November 2006 to May 2007, he was a Postdoctoral Scholar with the Department of Electrical and Computer Engineering, University of California, Davis. Currently, he is a Postdoctoral Research Associate

with the Department of Electrical and Systems Engineering, Washington University, St. Louis. His research interests are adaptive and statistical signal processing, including detection and estimation theory, optimization, distributed signal processing, sequential Bayesian inference, Monte Carlo methods, etc., and their applications in sensor arrays, communications, wireless networking, and biochemical sensors.



**Arye Nehorai** (S'80–M'83–SM'90–F'94) received the B.Sc. and M.Sc. degrees in electrical engineering from the Technion, Israel, and the Ph.D. degree in electrical engineering from Stanford University, Stanford, CA.

From 1985 to 1995, he was a faculty member with the Department of Electrical Engineering, Yale University, New Haven, CT. In 1995, he joined the Department of Electrical Engineering and Computer Science, The University of Illinois at Chicago (UIC), as Full Professor. From 2000 to 2001, he was Chair

of the Department of Electrical and Computer Engineering (ECE), which then became a new department. In 2006, he became Chairman of the Department of Electrical and Systems Engineering, Washington University, St. Louis (WUSTL). He is the inaugural holder of the Eugene and Martha Lohman Professorship and has been the Director of the Center for Sensor Signal and Information Processing (CSSIP) at WUSTL since 2006.

Dr. Nehorai was Editor-in-Chief of the IEEE TRANSACTIONS ON SIGNAL PROCESSING during 2000–2002. In 2001, he was named University Scholar of the University of Illinois. From 2003 to 2005, he was Vice President (Publications) of the IEEE Signal Processing Society, Chair of the Publications Board, member of the Board of Governors, and member of the Executive Committee of this Society. From 2003 to 2006, he was the founding editor of the special columns on Leadership Reflections in the *IEEE Signal Processing Magazine*.

He was corecipient of the IEEE SPS 1989 Senior Award for Best Paper with P. Stoica, coauthor of the 2003 Young Author Best Paper Award, and corecipient of the 2004 Magazine Paper Award with A. Dogandzic. He was elected Distinguished Lecturer of the IEEE SPS for the term 2004 to 2005, and received the 2006 IEEE SPS Technical Achievement Award. He is the Principal Investigator of the new multidisciplinary university research initiative (MURI) project entitled "Adaptive Waveform Diversity for Full Spectral Dominance." He has been a Fellow of the IEEE since 1994 and of the Royal Statistical Society since 1996.